Available online at www.sciencedirect.com

SCIENCE DIRECT®

Geomorphology 70 (2005) 112–128

GEOMORPHOLOGY

www.elsevier.com/locate/geomorph

Development of offset channels across the San Andreas fault

Shunji Ouchi*

College of Science and Engineering, Chuo University, 1-13-27 Kasuga, Bunkyo, Tokyo, 112-8551, Japan

Received 26 October 2004; received in revised form 19 April 2005; accepted 22 April 2005
Available online 8 June 2005

Abstract

The San Andreas fault offsets some small gullies incising the relatively flat surfaces in the Carrizo Plain, California. Among these gullies, those with larger drainage basins have larger offsets, probably because gullies that have larger floods can keep the channels entrenched and subjected to the fault displacement longer. On the other hand, older offset channels in the area, which have much larger offsets, indicate that the gradual shift to straighter courses seems probable only for offset channels able to keep and accumulate the offset for a long time. The strike-slip fault displacement offsets a channel as much as the channel can follow with some modification by fluvial processes until overbank floods at the upper bend induce channel avulsion to a straighter course, or until the channel is captured by the beheaded and abandoned downstream reach of the adjacent channel moved with the fault displacement. The offset channel promotes aggradation upstream from the upper bend, and this makes the channel increasingly susceptible to overbank floods. The older offset channels are confined in valleys, and this condition is apparently preventive of channel avulsion or capture. The strike-slip fault displacement also deforms longitudinal profiles of channels. Assuming that the elimination of discontinuities in the longitudinal profile is the main response of fluvial processes to the deformation by fault displacement, nearly continuous longitudinal profiles of some old offset channels seem to indicate the full adjustment, the condition in which no more changes will occur as a response to fault displacement until the next fault slip deforms them. The irregularities in longitudinal profiles of other offset channels indicate that the channel adjustment by fluvial processes may be occurring but not enough to eliminate the irregularities. An offset river can attain a continuous longitudinal profile if it has enough time to adjust its longitudinal profile after the fault displacement. Otherwise, the discontinuity reflecting a various degree of adjustment would remain in the longitudinal profile until channel avulsion or capture occurs. The degree of adjustment and the probability of channel avulsion or capture depend highly on the fluvial ability and condition of each river as well as the time after the deformation.

Keywords: San Andreas fault; Strike-slip fault displacement; Offset channel; Longitudinal profile; Deformation type; River adjustment

1. Introduction

Offset rivers have long been recognized as clear evidence of horizontal displacement on strike-slip faults (e.g., Lawson et al., 1908; Lensen, 1958;

* Fax: +81 3 3814 0955.
E-mail address: souchi@kc.chuo-u.ac.jp.

0169-555X/$ - see front matter © 2005 Elsevier B.V. All rights reserved.
doi:10.1016/j.geomorph.2005.04.004

Allen, 1962; Kaneko, 1965; Wallace, 1968), and the amount of channel offset has been combined with age control at several locations to estimate the rate of fault displacement (e.g., Matsuda, 1966; Keller et al., 1982; Sieh and Jahns, 1984). However, not all channels crossing active strike-slip faults are offset (e.g., Lensen, 1958; Allen, 1962; Wallace, 1968; Gaudemer et al., 1989; Huang, 1993). Allen (1962) noted that a flow direction nearly perpendicular to the strike of a strike-slip fault is an important condition for the preservation of stream offsets; otherwise, the stream will follow the zone of fault slip. Wallace (1968) considered stream size, vertical fault displacements, and stream capture along strike-slip faults as the key factors controlling channel morphology of offset rivers. Gaudemer et al. (1989) and Huang (1993), who studied offset rivers in California and China, respectively, both concluded that about half the stream channels crossing strike-slip faults showed no clear offset or deflection; that about three-fourths of the remaining streams are deflected in a direction compatible with the fault displacement; and that the rest showed the opposite deflection. Huang (1993) further inferred that the orientation of the hillslope relative to the fault plays an important role in determining channel course.

River forms are essentially the products of fluvial processes, and offset rivers show the effects of fluvial processes as much as the fault displacement. Examination of the response or adjustment of streams to fault displacements, therefore, is necessary in order to use measured channel offsets to estimate strike-slip fault displacement. However, distinguishing channel deformation associated with fault displacement from channel changes caused by fluvial processes is usually very difficult, and offset channels are often the only evidence of fault displacement. Ouchi (2004) conducted flume experiments in which the effect of fault displacement can be distinguished from those of fluvial processes, but these are not a reproduction of what happens in real streams. Although the experiments provide some guidance on how to analyze the response of streams to strike-slip fault motion, studies based on real field data are essential to improve our understanding of the effects of fault displacement on rivers. This study analyzes the field-measured planform geometry and longitudinal profiles of some channels offset by the San Andreas fault as a trial to define the manner of response or adjustment of streams to strike-slip fault displacement.

Some authors (e.g., Matsuda, 1966; Wallace, 1968; Gaudemer et al., 1989) have pointed out the positive correlation between the amount of river offset and the river's overall length or size. The relationship between offset length (D) and channel length from the fault up to the divide (L) described by Matsuda (1966) has been recognized widely in Japan as a surprisingly robust feature of offset channels (e.g., Okada, 1970; Ando, 1972); and the method of estimating the average slip rate of a fault from the value of D/L, based on a second correlation between D/L and the slip rates of some well-known faults (Matsuda, 1975), has been applied by many Japanese researchers (e.g., Okada and Sangawa, 1978; Fukui, 1981; Yoshioka, 1986; Uemura, 1988). Gaudemer et al. (1989) demonstrated a similar correlation between the apparent offset and the river length upstream from the fault for offset rivers crossing strike-slip faults in California. They measured offset length and river length on 1:250,000 maps (excluding "small streams" such as Wallace Creek) and inferred the slip rates of some faults in a manner similar to Matsuda (1975), using estimated rates of river elongation taken from the literature. The values of fault slip obtained were well above the rates generally accepted; and Gaudemer et al. (1989) concluded that the measured river offset did not indicate the actual tectonic displacement. However, this discrepancy may indicate that river "offsets" determined from 1:250,000 maps reflect factors other than fault displacement alone, besides the possibility that the estimated river elongation rate they employed may be inappropriate for the purpose. The good correlation between the apparent offset and river length may simply indicate that large rivers are more sparsely spaced. The relationship between D and L (measured on maps) for some offset rivers in Japan may also reflect something other than fault displacement, as Matsuda (1975) himself suspected. Channels exhibiting a clear horizontal displacement associated with strike-slip faulting are usually too small to permit the construction of accurate planview channel geometry or longitudinal profiles from topographic maps. The field-measured planform geometry and longitudinal profiles of offset channels are necessary also in this respect.

2. Geometry and geometrical analysis of offset channels

Horizontal fault displacement offsets a stream by dragging a reach on one side of the fault away from its upstream or downstream reach on the other side along the fault line. An "offset reach" is the reach connecting these divided upstream and downstream reaches (Ouchi, 2004) (Fig. 1). Actual offset channels do not show simple linear geometry because fluvial processes add many irregularities and round off sharp corners caused by the fault displacement. Determining the values of geometrical properties of offset channels, therefore, is often very difficult. The exact position of the fault crossing the offset channels is also difficult to determine. In order to geometrically analyze offset channels, regression lines of three separate channel sections are used in defining the upstream, offset, and downstream reaches, as schematically illustrated in Fig. 1. They are referred to as the upstream, offset, and downstream lines. Two lines parallel to the fault strike are drawn through the intersections of the offset line with the upstream and downstream lines, and referred to as the upper and lower fault lines (Fig. 1). The real fault is supposed to lie within the zone bounded by the upper and lower fault lines. The width of this zone or the distance between these two fault lines (W) is assumed to roughly represent the fault width. Huang (1993) defined the angle of deflection as the angle between the fault strike and the offset reach. This angle of deflection can be defined as the angle between the fault line and the offset line (θ in Fig. 1). Most of the channels crossing strike-slip faults are not exactly perpendicular to the fault trace and instead are oriented more or less diagonally. The angle between the upstream (or downstream) line and the line perpendicular to the fault line is referred to as the "crossing angle" in this study (λ, measured in the same direction as θ). The offset length, Δh, is assumed to correspond to the amount of horizontal fault displacement the channel has taken. In cases in which the fault displacement has a vertical component (Δv), this results in an "offset slope" ($S_o = \Delta v/\Delta h$) of the fault. Regression lines are also drawn on longitudinal profiles to obtain channel slopes of these three reaches. The offset channel parameters, namely offset length (Δh), angle of deflection (θ), offset slope (S_o), channel gradient (S_c), and crossing angle (λ), are calculated from these regression lines. The crossing angle of the upstream reach is usually different from that of the downstream reach probably because the channel before the offset is not necessarily straight across the fault line. Therefore, parameters such as Δh, S_c, S_o, and λ are calculated for the upper and lower fault lines separately. The original channel, represented by the downstream reach, is assumed to have been displaced from the upstream reach along the upper fault line. The channel represented by the upstream reach is assumed to have been displaced along the lower fault line. In the latter case, the upstream line is extended to the lower fault line, and the distance along the lower fault line from this intersection to the intersection with the downstream line is taken to be the horizontal component of displacement (Δh_d) (Fig. 1). The vertical component of displacement, Δv_d, is the height difference between the extrapolated upstream line and the downstream line at the lower fault line. The slope of the upstream line on the longitudinal profile along channel (S_{cu}) is taken to be the channel gradient here and the crossing angle is defined using the upstream line (λ_u). In short, the assumed displacement along the lower fault line is estimated from Δh_d, Δv_d, S_{cu}, and λ_u, although the actual calculations are performed with the equations of regression lines. The same procedure is repeated for the upper fault line using Δh_u, Δv_u, S_{cd}, and λ_d. Two

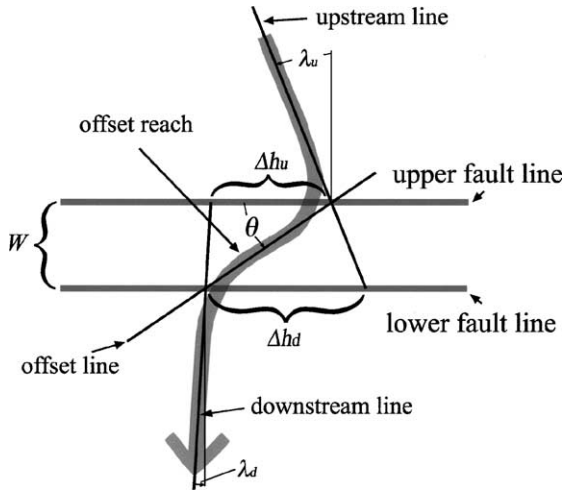

Fig. 1. A schematic diagram illustrating geometrical properties of offset streams and the method of measuring these properties. See the text for details.

values obtained for each parameter are considered to roughly indicate the range of the real value.

This estimation procedure was first applied to the experimental offset streams reported by Ouchi (2004). It gave reasonable results for all parameters except Δv. Although the experimental fault displacement had no vertical component, the estimated values of Δv range from 3 to 16 mm. This discrepancy is apparently due to the high rates at which the experimental streams obtain continuous longitudinal profiles mainly by downstream degradation. Downstream degradation (and upstream aggradation) due to the damming effect of the offset channel inevitably increases the Δv estimate. This overestimating tendency of Δv values should be considered in the analysis.

3. Measurement of offset channels crossing the San Andreas fault

The strike-slip displacement of the San Andreas fault in California and the offset channels that cross it have been well known for almost 100 years. Horizontal displacement that offset channels during the 1906 San Francisco earthquake was reported in detail shortly after the earthquake (Lawson et al., 1908). Wallace (1968) documented beautifully offset channels across the San Andreas fault in the Carrizo Plain, California, and these and other offset channels have been studied intensively since then as indicators of actual fault displacement (e.g., Sieh, 1978; Sieh and Jahns, 1984). In addition to these studies, numerous paleo-seismic studies have been carried out along the San Andreas fault in the area of central to southern California (e.g., Sieh, 1984; Weldon and Sieh, 1985; Sieh et al., 1989; Grant and Sieh, 1993, 1994; Grant and Donnellan, 1994). The accumulated knowledge of the fault activity and offset channels in this area provides a good starting point for more detailed analysis of river response to fault displacement. Moreover, the scarcity of vegetation and water flow in this area aids data collection in the field.

I measured planform geometry and longitudinal profiles of 10 channels crossing the San Andreas fault (9 in the Carrizo Plain and 1 near the Cajon Pass, southern California) (Fig. 2), which allowed detailed field measurement along their channel

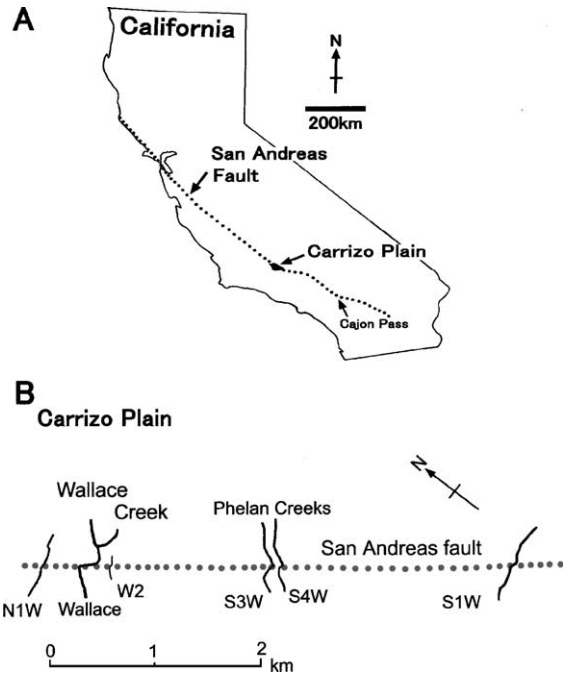

Fig. 2. Index map showing the locations of the Carrizo Plain and Cajon Pass, California (A), and location map of offset channels measured in the Carrizo Plain (B).

courses. Artificial channel modification and obstructions such as thorny vegetation and cattle fences, as well as discontinuous channels, restricted the number of measurements. All the field measurements were performed using a specially devised measuring instrument. The instrument consists of a pair of large dividers: the length of the line connecting the tips of two legs and its angle from the horizontal are automatically calculated from the opening angle of the legs (measured by tiltmeters set on the legs), the angle from vertical of one of the legs, and the length of each leg. The orientation is measured by a magnetic yaw-sensor attached on the instrument. The measured values are stored in a data logger each time a switch is pressed, and this was repeated while walking along a channel. Measurements were only made on reaches that were considered long enough to analyze the deformation caused by faulting. The strike of the fault was measured in the field using a Brunton compass when easily visible, and otherwise determined from topographic maps. For analytical convenience, magnetic orientations were exclusively used in this study. The data are plotted

in three graphs: planview, with the fault trace as the vertical axis; a projected longitudinal profile (longitudinal profiles projected onto the plane perpendicular to the fault trace); and a longitudinal profile along the channel (cf., Fig. 3). The upstream, offset, and downstream reaches, were defined on the planview diagram. The continuity of each longitudinal profile was also referred to when defining the separate reach segments. All the geometrical analyses were performed on these graphs and the calculated values of parameters are compiled in Table 1. Drainage area and channel length of each channel above the fault line measured on 1:24,000 topographic maps are also listed in the table.

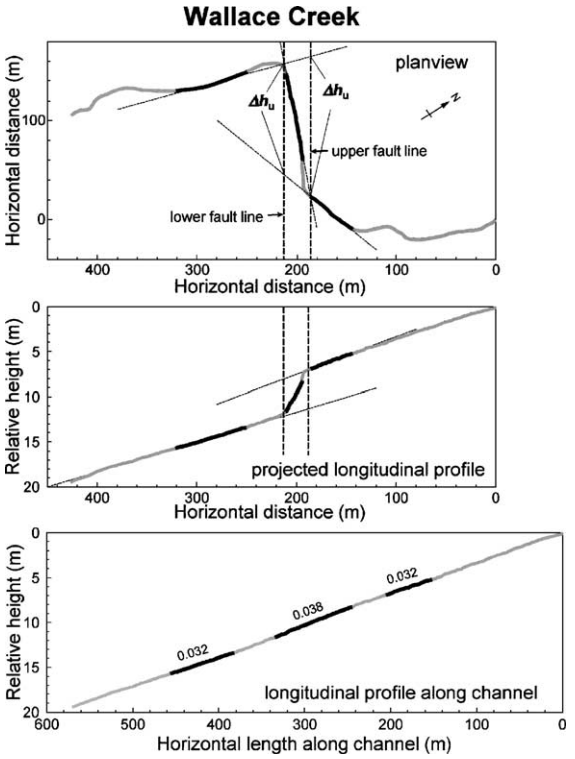

Fig. 3. Channel course geometry and longitudinal profiles of Wallace Creek in the Carrizo Plain, California. The vertical axis of the planview graph is parallel to the fault line. Dark lines correspond to the representative sections of the upstream, offset, and downstream reaches. The thin broken lines in the planview graph are regression lines of these sections, indicating upstream, offset and downstream lines. The projected longitudinal profile is the longitudinal profile projected onto the plane perpendicular to the fault trace. The numbers in the longitudinal profile along channel graph are the channel gradients of these three sections.

3.1. Carrizo Plain

Although I had intended to measure channels showing offsets at the fault, two of the nine channels measured in this plain appeared to show no clear offset at the fault trace in the planview diagram. One of them is considered to be a new gully that has developed since the last fault displacement. The second is a depositional channel on a small alluvial fan, which apparently *has* changed its course by channel avulsion since the last fault displacement. For the purpose of analyzing the effects of fault displacement, only those channels showing clear fault offsets in the planview diagram are reported on here (Fig. 2B).

Wallace Creek exhibits more than 100 m of dextral displacement at the trace of the San Andreas fault (Wallace, 1968; Sieh, 1978; Sieh and Jahns, 1984). Its offset reach is subparallel to the fault trace ($\theta \approx 9.6^\circ$), and the upstream and downstream reaches look parallel except for a relatively short reach immediately upstream from the fault (Fig. 3). This short reach, however, is in a shallow valley and appears to lie outside the fault zone: it is therefore considered here to be the upstream reach ($\lambda_u \approx -39^\circ$). Along the lower fault line, Δh is 113 m; and 141 m along the upper fault line. These values are comparable to that of 128 m measured by Sieh and Jahns (1984). The channel gradient ($S_c \approx 0.032$) is close to the offset slope ($S_o \approx 0.031$ at the upper fault line and 0.037 at the lower fault line). The offset reach is slightly steeper than the adjacent reaches.

A very small, shallow gully just SE of Wallace Creek by trail post 3 (labeled W2 in this study) has an offset reach gentler than that of the adjacent reaches (Fig. 4). Almost the entire offset is considered to have formed during the great Fort Tejon earthquake in 1857 (Sieh, 1978). The offset length Δh is 11–12 m, and S_o (0.005–0.023) is smaller than S_c (0.067–0.11). This small gully has a relatively large angle of deflection ($\theta \approx 24^\circ$) in spite of its minor ability to erode and the short time of adjustment after the displacement. Lateral shift of the offset reach can presumably occur rather easily within this shallow gully, but the small horizontal displacement across the fault zone probably contributed largely to the high angle of deflection.

Table 1
Measured and calculated properties of offset channels[a]

Offset stream		θ	λ	S_c	Δh (m)	Δv (m)	S_o	Average S_o/S_c	Deformation type	A (km^2)	L (m)	W (m)
Wallace	Upstream	9.6°	−39.2°	0.032	141.5	4.3	0.031	1.05	B	6.71	6889	26.3
	Downstream		15.5°	0.032	112.6	4.1	0.036					
W 2	Upstream	23.7°	−5.8°	0.067	12.0	0.06	0.005	0.19	A	0.03	389	5.3
	Downstream		0.2°	0.107	11.4	0.3	0.023					
S3W	Upstream	19.8°	7.3°	0.039	13.6	0.5	0.033	0.80	A	0.45	2307	5.7
	Downstream		−22.7°	0.038	16.7	0.5	0.027					
S4W	Upstream	21.0°	7.3°	0.032	21.3	0.6	0.030	0.95	B	1.95	4157	7.1
	Downstream		20.4°	0.037	19.5	0.7	0.035					
S1W	Upstream	22.1°	15.5°	0.044	27.2	1.0	0.036	0.90	B	4.12	6988	11.3
	Downstream		−2.2°	0.030	30.3	0.8	0.026					
N1W	Upstream	34.4°	−11.2°	0.036	14.3	0.5	0.033	0.84	–	0.91	2095	15.2
	Downstream		−27.4°	0.036	19.2	0.5	0.028					
N1H	Upstream	12.3°	−39.3°	0.077	119.3	6.5	0.055	0.74	A	0.08	484	35.4
	Downstream		−50.4°	0.065	132.8	6.5	0.049					
Cajon	Upstream	2.6°	−26.4°	0.077	91.5	6.9	0.076	1.06	B	0.58	1879	4.4
	Downstream		−45.8°	0.066	93.9	7.0	0.075					

See the text for details.

[a] θ: angle of deflection; λ: crossing angle; S_c: channel gradient; Δh: offset length; Δv: vertical offset; S_o: offset slope; A: drainage area above the fault; W: distance between the lower and the upper fault lines. Note that S_{cd}, λ_d (downstream row) and Δh_u, Δv_u (upstream row) are used to calculate S_o for the upper fault line (downstream row), and S_{cu}, λ_u (upstream row) and Δh_d, Δv_d (downstream row) for the lower fault line (upstream row).

Two neighboring gullies cutting a flat surface about 1.6 km SE from Wallace Creek (Phelan Creeks; labeled S3W and S4W in this study; Fig. 2B) show clear offsets along the trace of the fault (Fig. 4). They look very similar, but S3W is smaller than S4W. The offset length (Δh) is 14–17 m for S3W and 19–21 m for S4W. Sims et al. (1989) measured the offset of these gullies as 15.8 ± 0.6 m and 17.4 ± 1.6 m, respectively. Considering the difference in the procedure of measurement, the values are compatible. The angle of deflection θ is 20° for S3W and 21° for S4W. The wide ranges of λ (−23~7° for S3W and 7–20° for S4W) suggest curved channel courses before the fault displacement.

A gully about 4 km SE of Wallace Creek (S1W) has a relatively large offset ($\Delta h \approx 27$–30 m), with $\theta \approx 22°$ and $\lambda \approx -2$–15° (Fig. 5). The offset reach runs through a gap in a low ridge-like mound that has formed along the fault. This feature probably acted to preserve the channel's offset. Another small gully (N1W), about 400 m NW of Wallace Creek, has a short offset ($\Delta h \approx 14$–19 m) and a large angle of deflection ($\theta \approx 34°$) with $\lambda \approx -11$ to −27° (Fig. 5). The values of S_o and S_c are similar.

A relatively deep gully north of Hanline Ranch near the southern end of the Carrizo Plain (N1H) exhibits a large dextral offset ($\Delta h \approx 119$–133 m) with sharp bends ($\theta \approx 12°$ and $\lambda \approx -50$ to −39°) (Fig. 6). This gully may be a young feature that has developed in a small older valley. The channel geometry, however, indicates that the valley itself is offset by the San Andreas fault.

3.2. Cajon Pass

A small tributary of Prospect Creek near Cajon Pass, north of San Bernardino in southern California (labeled Cajon in this study), undergoes an abrupt dextral offset across the San Andreas fault (e.g., Weldon and Sieh, 1985; Weldon, 1987). Its offset is large ($\Delta h \approx 92$~94 m) and the angle of deflection rather small ($\theta \approx 2.6°$) (Fig. 6). In contrast to the gullies in the Carrizo Plain, this stream flows down a relatively large valley with more extensive vegetative cover, and the channel course contains many small irregularities because of large gneiss or granite boulders on the channel floor. The valley and the channel look to be older than the gullies in the Carrizo Plain. Its smooth longitudinal

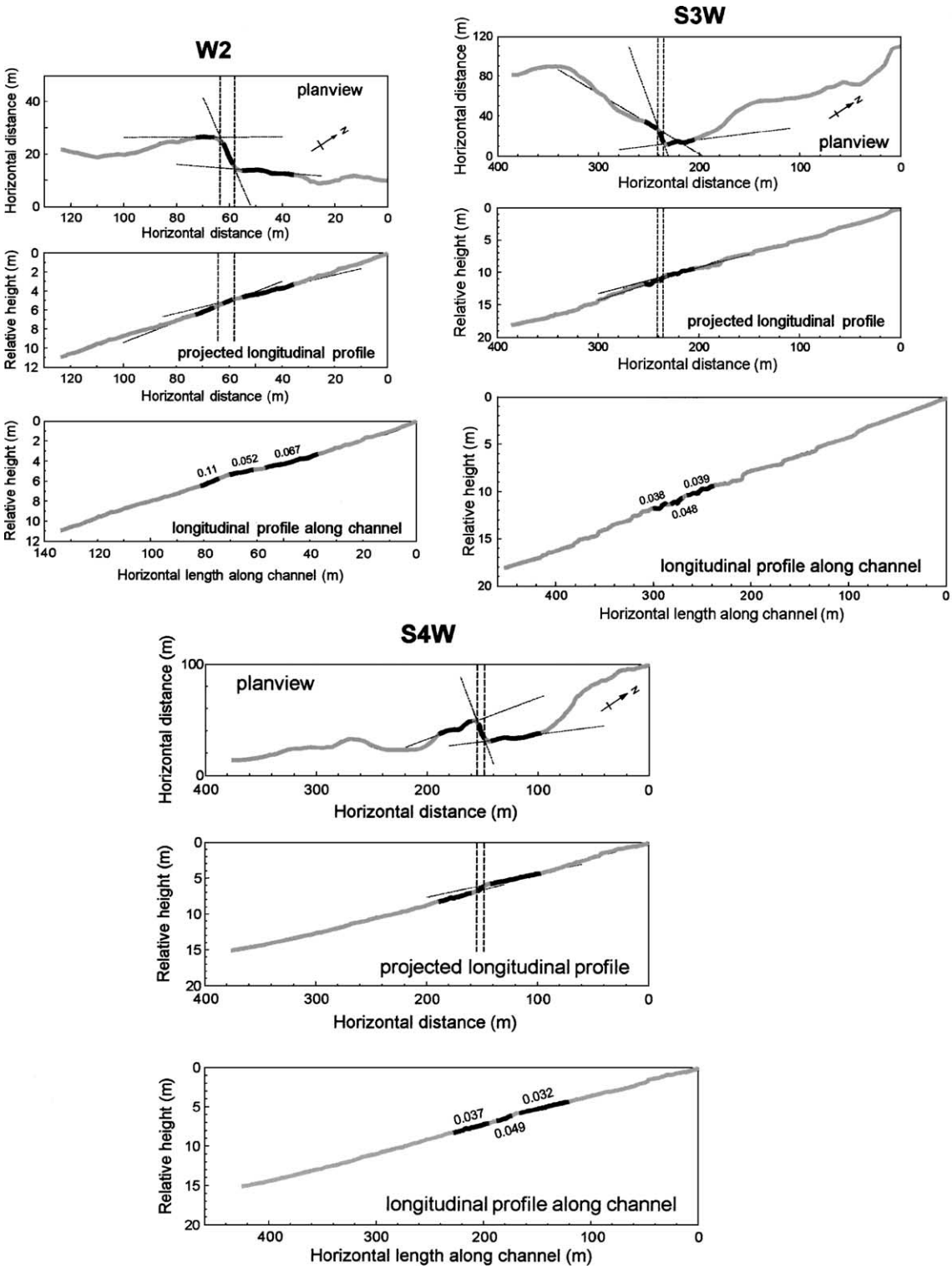

Fig. 4. Channel course geometry and longitudinal profiles of small offset gullies (W2, S3W and S4W) in the Carrizo Plain. See Fig. 3 for details.

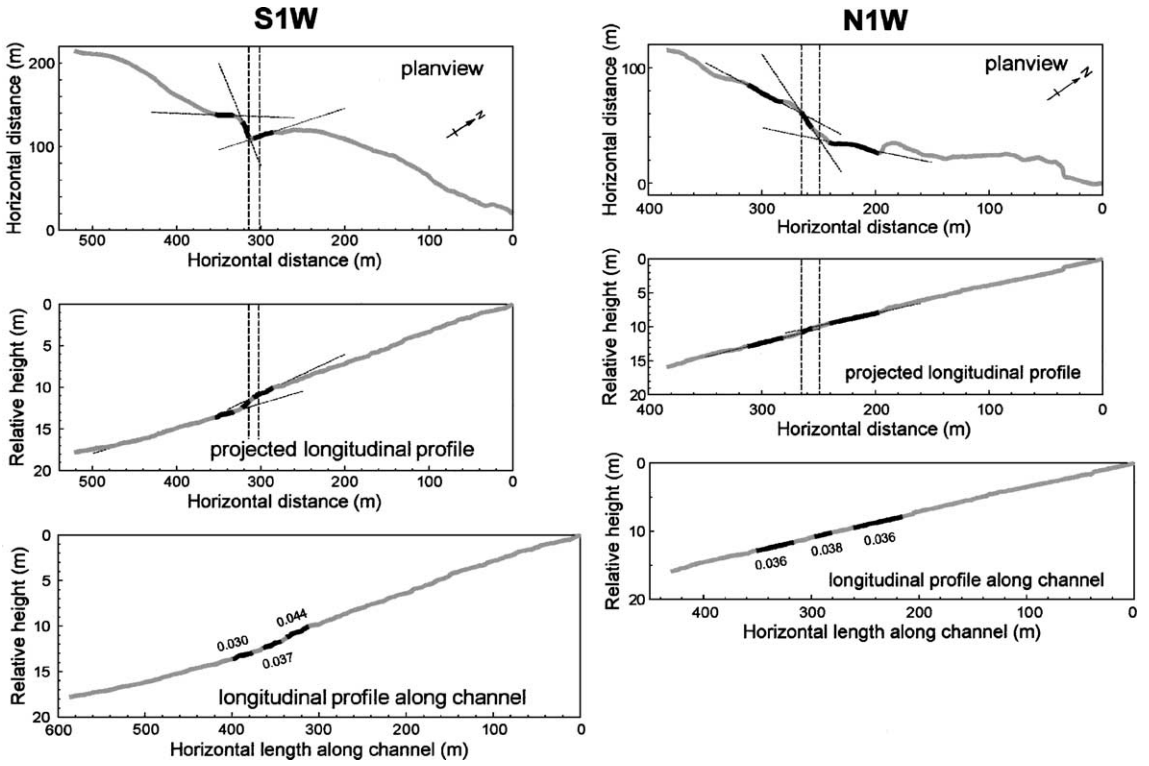

Fig. 5. Channel course geometry and longitudinal profiles of small offset gullies (S1W and N1W) in the Carrizo Plain. See Fig. 3 for details.

profile along channel suggests the progress of fluvial adjustment.

4. Discussion

4.1. Planform geometry of offset channels

All eight channels reported here show apparent horizontal offset along the fault trace in the direction of fault displacement. However, a closer look at these small gullies reveals that the offsets of N1W and S3W may not be the direct and simple result of fault displacement. These two small gullies both have larger gullies on their left (SE) side and the beheaded and abandoned channels of these larger gullies, which moved with fault displacement, possibly captured the upstream reaches of the gullies. The downstream reach of N1W is actually defined as an old abandoned channel of Wallace Creek by Sieh and Jahns (1984). Judging from its course close to the larger gully of S4W on the left, the small gully labeled S3W may have once been a tributary of S4W merging below the fault trace. It was then possibly captured by the abandoned downstream channel of S4W coming close to the upstream reach. The gully of S3W may have taken a short quasi-offset course in the opposite direction to the fault slip when S4W took a relatively straight course across the fault trace with channel avulsion and abandoned the old offset channel. The abandoned channel will be gradually filled up with materials carried by surface wash. Stream flows from the upstream catchment area are necessary to keep the gully entrenched. When a beheaded and abandoned channel captures the adjacent channel before being completely filled, the channel reactivates and may show a quasi-offset course in the direction that is the same or opposite to the fault slip depending on the relative position of the abandoned channel. In this case, the offset length Δh does not correspond to the amount of fault slip at the channel. The difference in offset length between S3W ($\Delta h \approx 14$–17 m) and S4W ($\Delta h \approx 19$–21 m) is not necessarily explained by the difference in the

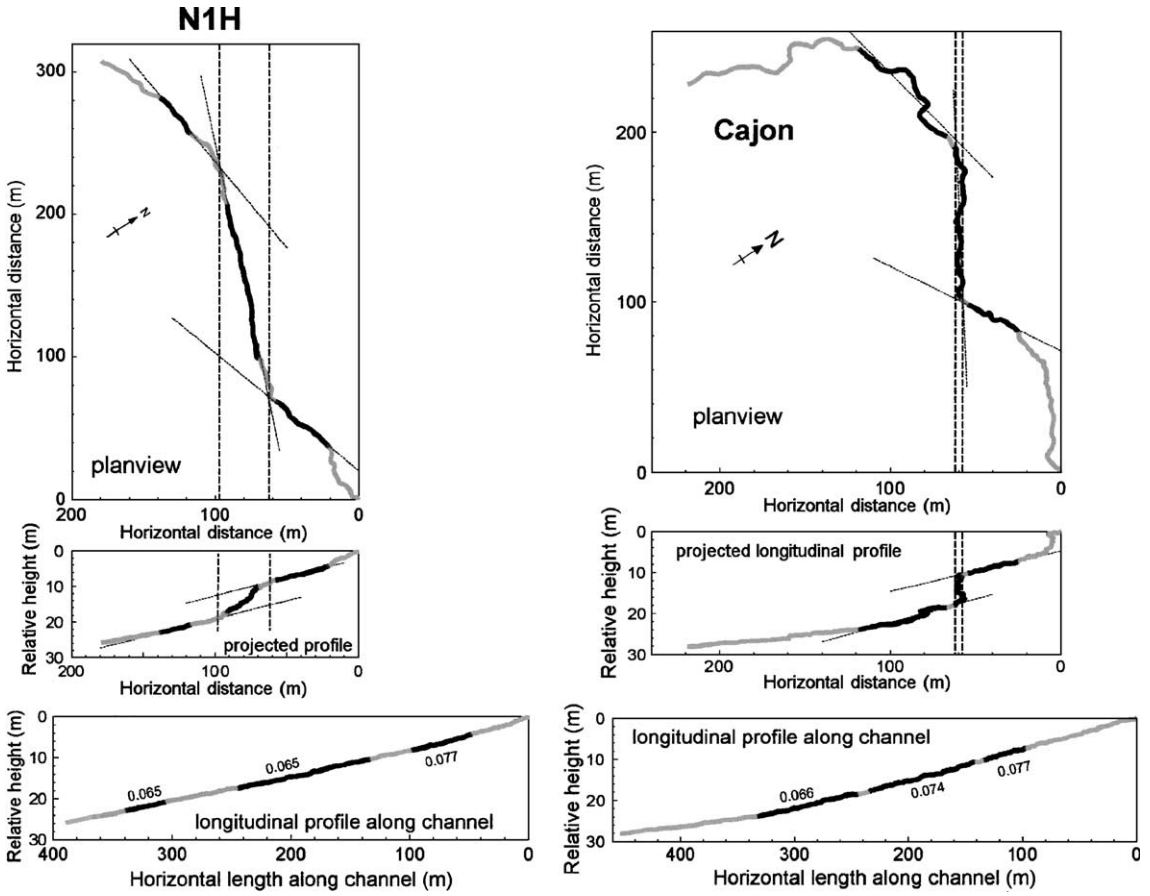

Fig. 6. Channel course geometry and longitudinal profiles of N1H and Cajon. See Fig. 3 for details.

amount of fault displacement that the gullies have taken.

Fig. 7 illustrates the relationship between offset length (Δh) and drainage area above the fault trace (A). In this diagram, points representing small gullies cutting relatively flat surfaces of pediments or alluvial fans in the Carrizo Plain align nicely along a line, whereas other points scatter above. The line is the regression line for small offset gullies in the Carrizo Plain (W2, S1W and S4W) excluding N1W and S3W. Points representing N1W and S3W are slightly off the line. The unrealistic y-intercept of the regression line (12.6 at $A=0$) is apparently caused by the intermittent increase in offset length (Δh) with earthquake-inducing fault slips. Although the amount of data is too small to be statistically significant, the tendency that a gully of longer offset

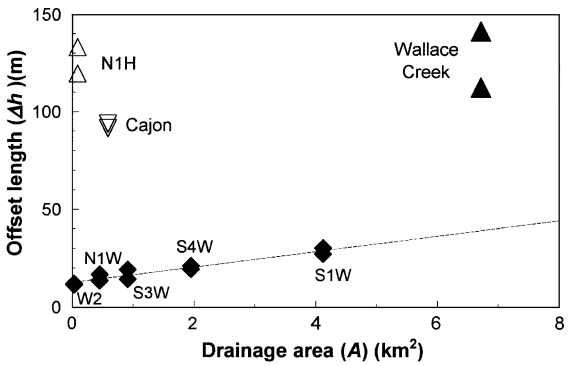

Fig. 7. Relationship between offset length (Δh) and drainage area above the fault line (A). The regression line (broken line) is drawn for the plots of W2, S4W and S1W. The equation is $y=3.96x+12.6$ and $R^2=0.93$.

length has larger drainage area is apparent for the small offset gullies in the Carrizo Plain. A simple interpretation of this tendency is that these small gullies have been offset by the fault while their drainage basins were expanding. Accepting this interpretation, the fault slip rate of 33.9 ± 2.9 mm year^{-1} estimated by Sieh and Jahns (1984) in this area can be translated into a drainage area expansion rate of 7.8–9.3 km^2 kyr^{-1}. This interpretation, however, is inappropriate. Gullies (or arroyos) in semi-arid western North America are known for a history of entrenching and filling due to short-term climatic changes and/or to land use changes by humans (e.g., Peterson, 1950; Bull, 1997). These gullies are hardly regarded as a lasting feature developed with drainage basin expansion. The gullies in this plain probably have entrenched and filled repeatedly without major changes in their drainage area. Bull (1997) pointed out that a channel entrenches where stream power exceeds the resistance of the valley floor, and stream power increases with discharge whereas valley floor resistance does not change largely in the same area. He considered that trunk channels (with larger drainage area) remain entrenched longer than headwater channels. Drainage area is sometimes considered as a possible substitute for discharge (e.g., Hack, 1957). Hack (1973) devised an easily obtainable index reflecting stream power, "gradient index" or **SL** index. The **SL** index is the product of the local slope (**S**) and the stream length from the drainage divide measured along the channel (**L**). Taking the channel length from the fault line to the drainage divide (L) as **L** and S_c as **S**, the value of $S_c \times L$ is equivalent to the **SL** index. The relationship between offset length (Δh) and $S_c \times L$ illustrated in Fig. 8, which looks similar to Fig. 7, indicates that among small offset gullies in the Carrizo Plain, a gully with larger stream power has longer offset; in other words, a gully with larger stream power can keep its channel entrenched longer. The correlation between Δh and A in Fig. 7 is also considered to simply indicate that a larger drainage basin keeps the gully entrenched longer.

The Carrizo segment of the San Andreas fault is recognized as a strong fault segment (e.g., Sieh and Jahns, 1984; Grant and Sieh, 1994), which releases the shear strain accumulated during a long recurrence interval with a sudden fault slip, inducing a large

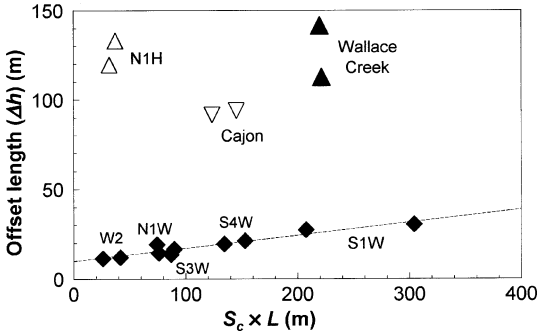

Fig. 8. Relationship between offset length (Δh) and SL index ($S_c \times L$). The regression line (broken line) is drawn for the plots of W2, S4W and S1W. The equation is $y = 0.07x + 10.0$ and $R^2 = 0.91$.

earthquake. The fault slip of the Carrizo segment at the time of the latest large earthquake in 1857 (Fort Tejon earthquake) is estimated as 9.5 ± 0.5 m (Sieh and Jahns, 1984) at Wallace Creek and 11.0 ± 2.5 m across a greater width of the fault zone (Grant and Donnellan, 1994). The offset of small gullies in the Carrizo Plain can possibly be explained by three large fault slips associated with earthquakes including the last fault slip at the time of the Fort Tejon earthquake. The offset of W2 ($\Delta h \approx$ 11–12 m) apparently reflects this last fault slip, and the offset of S4W ($\Delta h \approx$ 19–21 m) is due probably to the last and the penultimate fault slips. The longest Δh of S1W (27–30 m) indicates the accumulation of three large fault slips. Sieh and Jahns (1984) estimated the fault slip associated with the last three earthquakes as 9.0 ± 0.5, 12.3 ± 1.2 and 11.7 ± 2.2 m at Wallace Creek, and Grant and Sieh (1993) as 7, 8–9 and 5–6 m at the Phelan fan from stratigraphic evidence and radiocarbon dating. The lengths of channel offset by these three fault slips estimated in this study (11–12, 7–10 and 6–11 m, respectively) are compatible with the values of fault slips, considering the modification by fluvial processes. Sieh and Jahns (1984) estimated the dates of two earthquakes in this area prior to 1857 as 1540–1630 and 1120–1300 and Grant and Sieh (1994) as 1405–1510 and 1277–1510 at the Bridart fan about 5.5 km SE from Wallace Creek. These dates suggest that the gully of S1W started to entrench sometime before 1100–1500 and S4W around 1400–1600.

Other offset channels with longer offset length (namely Wallace Creek, N1H, and Cajon) show no

correlation between Δh and A or $S_c \times L$ (Figs. 7 and 8). Their offset reaches are not gullies cutting the flat surfaces of pediments or alluvial fans, but they are channels confined in valleys in a somewhat hilly part of the area. Their longer offset length means that these offset channels have existed longer than the gullies cutting flat surfaces in the Carrizo Plain. Huang (1993) assumed that the angle of deflection increases with time as a consequence of the horizontal shift of the offset reach. He apparently considered the increase in the angle of deflection to be a means of channel adjustment to deformation by horizontal fault displacement. In this case, offset length (Δh) and the angle of deflection (θ) would show a positive correlation. However, the smaller/younger gullies in the Carrizo Plain, which have a positive correlation between Δh and A or $S_c \times L$, show no correlation between Δh and θ (Fig. 9). For the older offset channels (Wallace Creek, N1H, and Cajon), on the other hand, θ increases with Δh (Fig. 9). This tendency suggests that the angle of deflection (θ) gradually increase with offset length (Δh) only for the channels which could accumulate their repeated offset for a long time. Taking the fault width into account, young offset channels can have large angles of deflection because of their short offset length. If the increase in θ by lateral shift of the offset reach does not occur, θ will inevitably decrease as Δh increases. The old offset channels with longer offset length have smaller θ than young gullies (Fig. 9), and this probably reflects the decrease in θ due to the increase in Δh without a significant increase in θ

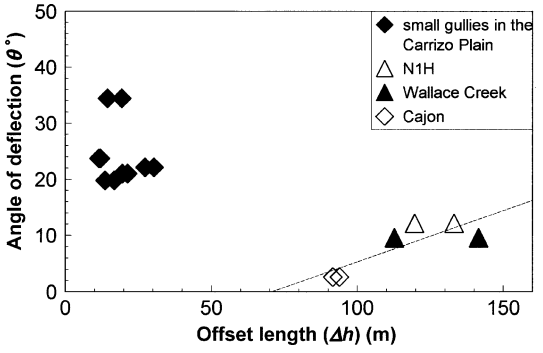

Fig. 9. Relationship between the angle of deflection (θ) and offset length (Δh). The broken line in the diagram is a regression line for the plots of old offset channels (Wallace Creek, N1H and Cajon). The equation is $y=0.18x-13.0$ and $R^2=0.68$.

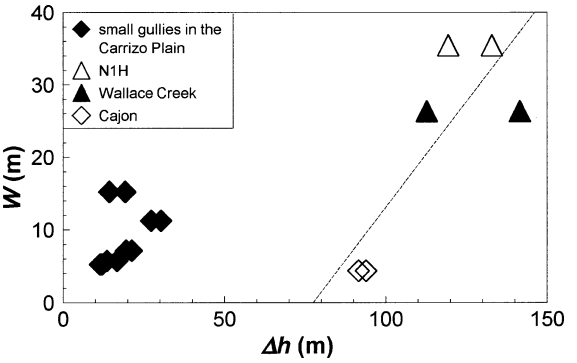

Fig. 10. Relation of the distance between upper and lower fault lines (W) to offset length (Δh). The broken line in the diagram is a regression line for the plots of old offset channels. The equation is $y=0.58x-45.1$ and $R^2=0.68$.

by lateral channel shift. The fault width, which is another variable determining the value of θ, is assumed here not to change with Δh. Robertson (1983) indicated, based mainly on the observations in mines, that the thickness of gouge and breccia on a fault increases with its displacement. Although Robertson (1983) excluded large strike-slip faults, his statement means that fault width may possibly increase with fault displacement. The offset length (Δh), however, is a variable indicating the amount of channel offset, not the whole amount of fault displacement. Offset channels crossing the same fault strip can have a variety of offset lengths. Offset channels reported in this study are all crossing the San Andreas fault and the fault width does not differ with Δh. The distance between the upper and lower fault lines (W) as a substitute for fault width shows no correlation with Δh as a whole (Fig. 10), although W shows some increase with Δh for older offset channels. The increment of Δh required to reduce a certain amount of θ will increase rapidly when θ becomes small or Δh becomes long, because Δh increases with the decrease in θ ($0<\theta<90^\circ$) as a cotangent function. Therefore, even a slight increase in θ by the lateral shift of the offset reach can surpass the decrease in θ associated with the increase in Δh when the channel offset becomes large enough. The narrow fault width possibly enhances this effect. The weak positive relationship between Δh and θ for old offset channels shown in Fig. 9 probably indicates this gradual increase in θ. The slight positive correlation of W with Δh for these old

offset channels (Fig. 10) is also considered to reflect this increase in θ by the lateral channel shift.

The fault slips offset a channel as much as the channel can follow with some modification, until a large flood induces channel avulsion to a straighter course, or until the beheaded and abandoned downstream reach of the adjacent channel moved with the fault block captures the channel. The process of deformation and adjustment then resumes and repeats all over again. The older offset channels are confined in valleys, and this condition is apparently preventive of channel avulsion or capture. Some channels can keep and accumulate channel offsets for a long time, and in this case, we can probably consider the increase in the angle of deflection as a channel adjustment by fluvial processes.

4.2. Deformation and adjustment of longitudinal profiles

The effects of tectonic movements on rivers have been discussed mainly with regard to longitudinal profiles and particularly as the cause of longitudinal profile "anomalies" (e.g., Burnett and Schumm, 1983; Seeber and Gornitz, 1983; Keller and Rockwell, 1984; Rockwell et al., 1984; Ouchi, 1985; Bull and Knuepfer, 1987; McKeown et al., 1988; Wells et al., 1988; Merritts and Vincent, 1989; Rhea, 1989; Willemin and Knuepfer, 1994; Zuchiewicz, 1995; Burbank et al., 1996; Benito et al., 1998; Demoulin, 1998; Harbor, 1998). These tectonic movements that produce local convexity or concavity in longitudinal profiles are usually vertical-uplift, subsidence, or tilting. Snow and Slingerland (1990) suggested, based on numerical experiments, that these anomalies in stream profiles are in some cases the expression of dynamic equilibrium between fluvial processes and tectonic movements. Burbank et al. (1996) concluded that large rivers, such as the Indus, can attain equilibrium profiles wherein local fluvial gradients are adjusted until incision rates balance the bedrock uplift rate. Harbor (1998) considered that the Sevier River, Utah, is responding to an active uplift by transporting just about the amount of sediment required to maintain the deformed convex-up profile, an expression of dynamic equilibrium. The horizontal offset caused by strike-slip faults is generally *not* considered to deform longitudinal river profiles. However, this is not necessarily true, and horizontal offset does cause the longitudinal profiles of streams to change. Longitudinal profiles of offset rivers are also interpreted to reflect the interaction between fluvial processes and deformation associated with fault displacement. In the discussion on the planform geometry of offset channels, offset channels are regarded as channels deformed by fault displacement, and dynamic equilibrium between fluvial processes and fault displacement can hardly be imagined. Longitudinal channel profiles are considered to reflect fluvial processes better than the planform geometry, and profiles may show the interaction between fluvial processes and fault displacement better.

The horizontal displacement of a strike-slip fault elongates the longitudinal profile of a channel by adding a new section. Taking the vertical component of fault displacement into account, the deformation of longitudinal profiles can be classified into three types based on the relationship between the fault displacement and the channel gradient (Fig. 11). Type A describes the deformation when the ratio of the vertical component of fault displacement to the horizontal component (offset slope) is less than the channel gradient. The offset slope equals the channel gradient for Type B and exceeds it for Type C. Fault displacement creating a reverse slope (in which the relative motion of the downstream block is upwards) is considered as an extreme case of Type A deformation. This extreme case is probably uncommon because small rivers generally follow the slope created by the long-term average of tectonic movements. Type A deformation is expected to occur where vertical fault displacement is small and/or channel gradients are high. Large vertical displacements and/or low stream gradients can cause Type C deformation. In the flume experiments, offset streams seemed to halt further adjustment once they had attained mostly continuous longitudinal profiles by eliminating the discontinuity caused by the fault displacement (Ouchi, 2004). Offset streams with Type B deformation, for which the gradient of the original offset reach can be similar to the channel gradient, are likely to require minimum channel adjustments. The experiments also suggested that the horizontal channel offset act as a dam, inducing upstream aggradation and downstream degradation, although the experimental stream without sediment supply actually promoted downstream

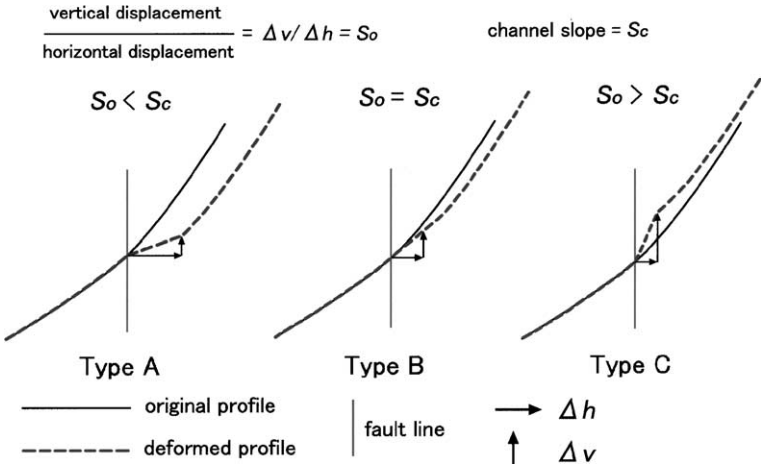

Fig. 11. Types of longitudinal channel profile deformation caused by strike-slip faults.

degradation more. For offset streams experiencing Type A deformation, which tends to create an offset reach of a shallower gradient than the original channel gradient, vertical adjustment supposedly proceeds easily by upstream aggradation and downstream degradation, but the upstream aggradation makes the channel increasingly susceptible to overbank floods. Offset streams of Type C, on the other hand, would appear to require the greatest adjustment to reach a continuous gradient. However, this type of channel offset promotes out-of-bank floods at the upper bend and may induce more frequent channel avulsion.

One of the offset channels excluded from the previous discussion, S3W, can be included in the discussion on the deformation and adjustment of longitudinal profiles, because S3W was apparently offset by fault slips, at least by the fault slip associated with the large earthquake in 1857. Judging from the gully size and the fault slip length, deformation by fault slip is probably a prominent feature in its longitudinal profile. On the other hand, another offset channel excluded from the previous discussion, N1W, is better excluded from the discussion. The capture by the beheaded and abandoned channel of much larger Wallace Creek may overwhelm the effect of fault displacement on the longitudinal profile of N1W.

The deformation type of each offset channel is estimated from the values of S_c and S_o. When the estimated offset slope (S_o) is less than the channel gradient (S_c), the deformation type of the offset channel is Type A. The offset slope equals the channel gradient for Type B and exceeds it for Type C. Each offset channel has two sets of S_o and S_c values for the upper and lower fault lines, but for convenience the channel deformation type is judged by the average value of S_o/S_c. An average value within the range of 1.1–0.9 is considered here to indicate Type B deformation. An average value smaller than that range represents Type A, and larger represents Type C. All the offset channels reported in this study, except for N1W, are inferred to have undergone Type A or Type B deformation (Table 1). The value of S_o (and therefore S_o/S_c), however, is usually overestimated due to the downstream degradation and/or upstream aggradation promoted by the channel offset. Experimental offset streams, for example, were all estimated to have Type C deformation, although their actual deformation by the simple horizontal fault displacement was Type A. In the experiments, the lack of sediment supply particularly promoted downstream degradation with the damming effect of an offset course, and the resultant shallow gradient of the downstream reach enhanced the tendency of overestimating S_o and converted the estimate of deformation type from Type A to Type C. The method of estimating the deformation type from contemporary longitudinal channel profiles has to be applied while taking account of the strong possibility of overestimating S_o. The offset channels estimated as Type A by the method employed here, therefore, certainly have Type A deformation, and those estimated as Type B have possibly undergone Type A deformation. Sieh and Jahns (1984) estimated

the vertical component of fault displacement at Wallace Creek to be 2.3% of the lateral component (i.e., S_o=0.023) for the past 3800 years, based on the deformation of river terraces. Weldon and Sieh (1985) estimated the lower rate of <0.015 for the old fluvial deposit at Cajon Creek. The values of S_c of the offset channels reported here are all above these rates (Table 1), suggesting Type A deformation for all the channels. However, Wallace Creek, S1W, S4W and Cajon are judged Type B. All these offset channels judged Type B have larger values of $S_c \times L$ than those judged to be Type A (Fig. 8). I speculate that the original channel deformation by the San Andreas fault is Type A for all offset channels reported here, but channels with more effective fluvial processes (or larger stream power) transform the apparent deformation type from Type A to Type B.

As the flume experiments suggest, trying to eliminate discontinuities in the longitudinal profile is probably the main response of fluvial processes to channel offset by fault displacement. Two of the old offset channels, N1H and Cajon, have nearly continuous longitudinal profiles along the channel (Fig. 6), which indicates the elimination of discontinuities in longitudinal profiles (or full adjustment) by fluvial processes. These offset channels apparently have a longer time since the last deformation by fault slip, and will not show any more changes as a response to the fault displacement until deformed by the next fault slip. The longitudinal profile along the channel of the smallest offset channel, W2, clearly shows deformation of Type A (Fig. 4). As the smallest and youngest offset channel, W2 apparently did not have enough time and fluvial ability to eliminate the discontinuities in its longitudinal profile caused by fault slip. Other offset channels in the Carrizo Plain (Wallace Creek, S1W, S3W and S4W) show some irregularities around offset reaches in their longitudinal profiles along channel (Figs. 3–5). The offset reach or the upstream bend segment tends to have a higher gradient and this gives a slight local convexity to the longitudinal profile along channel. These discontinuities in longitudinal profiles, which look different from the Type A deformation like W2, indicate that channel adjustment by fluvial processes is occurring, but not enough to eliminate discontinuities. The higher gradient of the offset reach or the upstream bend segment is probably derived from the damming effect of the offset channel, upstream aggradation and downstream degradation. An increase in the angle of deflection can also have an effect of making the offset reach steeper. Upstream aggradation seems especially important for offset channels in the Carrizo Plain. Unlike the flume experiment, a considerable amount of sediment is certainly transported in these channels during floods, although they are highly intermittent and ephemeral. Deposition would easily occur upstream of the upper bend, causing a higher channel gradient on the downstream segment against the Type A deformation of the longitudinal profile. Discontinuity of this type in the longitudinal profile indicates that the channel is responding to deformation by fault displacement. The discontinuity will be erased with the advance in fluvial adjustment, but the aggradation in the upstream reach will make the channel susceptible to overbank floods and will finally cause channel avulsion. For offset streams confined in valleys, this avulsion will not occur easily and the channels can accumulate the offset by fault displacement longer. The concept of equilibrium between fluvial and tectonic processes does not seem valid for the longitudinal profiles of small offset rivers reported in this study.

5. Summary and concluding remarks

Channel geometries and longitudinal profiles of some offset channels crossing the San Andreas fault in the Carrizo Plain and near the Cajon Pass, southern California, were measured in the field, and represented on diagrams of planview, projected longitudinal profile and longitudinal profile along channel. Despite the intention to select channels offset by the fault, two of the ten measured channels appeared to show no clear offset at the fault trace in the planview diagram. They are either a new gully developed since the last fault displacement or a depositional channel on a small alluvial fan, which probably *has* changed its course by avulsion recently. Even among the channels showing apparent offsets at the fault trace, two are considered to be channels captured by the beheaded and abandoned downstream reaches of adjacent larger channels. Considering the number of channels excluded from the measurement, it is apparent that the majority of channels crossing the San Andreas fault do not show clear offset by the fault.

This seems to confirm the observation by Gaudemer et al. (1989) and Huang (1993). Whether a channel crossing a strike-slip fault shows a clear offset by the fault displacement depends heavily on the history and fluvial conditions of the channel.

The geometric properties of the offset channel, such as the angle of deflection (θ), offset length (Δh), channel gradient (S_c), and offset slope (S_o), were calculated from regression lines through the upstream, offset, and downstream reaches. Drainage area (A) and channel length (L) above the fault were measured on topographic maps. Small offset gullies cutting the relatively flat surfaces of pediments or alluvial fans in the Carrizo Plain show a positive correlation between Δh and A or $S_c \times L$, which is a possible substitute for stream power. This correlation seems to confirm the interpretation that a stream of larger stream power has a greater ability to keep the channel entrenched, and therefore subjected to the fault displacement, for a longer time. On the other hand, older channels with larger offsets and smaller angles of deflection, which are confined in valleys, show a slight increase in θ with Δh. The gradual shift of the offset channel to a straighter course seems probable only for the offset channels that could keep and accumulate the offset for a long time. The confinement in valleys apparently allowed these channels to keep and accumulate their offset for a much longer time than the young gullies.

The deformation of longitudinal profiles by strike-slip faulting can be classified into three types based on the relative magnitudes of the fault displacement slope (offset slope; S_o) and the channel gradient (S_c). Type A deformation occurs when S_o is smaller than S_c, Type B when the two are equal, and Type C when S_o is steeper than S_c. Although the known offset slope of the San Andreas fault is lower than channel gradients of all measured offset channels (Type A), some offset channels that have larger values of $S_c \times L$ are classified as Type B. Offset slopes of the fault estimated from present channels tend to be larger due to the damming effect of the channel offset (upstream aggradation and downstream degradation) especially for channels of higher fluvial ability.

Assuming that eliminating discontinuities in the longitudinal profile is the main response of fluvial processes to channel deformation by fault displacement, nearly continuous longitudinal profiles of two old offset channels (N1H and Cajon) seem to indicate the state of full adjustment, the condition in which further changes as a response to fault displacement will not occur until the next fault slip deforms them. Other offset channels show some irregularities in their longitudinal profiles around their offset reaches. These irregularities indicate that channel adjustment by fluvial processes may be occurring, but not enough to eliminate the irregularities. The strike-slip fault displacement is considered to offset a channel as much as the channel can follow with some modification by fluvial processes, until overbank floods at the upper bend induces channel avulsion to a straighter course. Upstream aggradation as an effect of the channel offset will make the channel susceptible to overbank flooding. The process of deformation and adjustment then resumes all over again unless stream capture by the adjacent channel occurs. The older offset channels are confined in valleys, and this condition is apparently preventive of channel avulsion or capture. If an offset river has enough time to adjust the longitudinal profile by itself after the fault displacement, it can attain a continuous longitudinal profile regardless of the planform channel geometry, which may show a slight increase in the angle of deflection. Otherwise, the discontinuity reflecting a various degree of adjustment would remain in the longitudinal profile until channel avulsion or capture occurs. Offset rivers seem to be mostly in the process of adjustment after the almost instantaneous deformation by fault displacement, unless channel avulsion or capture occurs. The degree of adjustment and the probability of channel avulsion or capture depend highly on the fluvial ability and condition of each river as well as the time after the deformation. The concept of equilibrium between fluvial and tectonic processes is apparently not necessary here. The discussion on the equilibrium between fluvial and tectonic processes can probably be held better at a larger scale of time and space, but the reexamination of the effectiveness of equilibrium between these two fundamentally different processes might be an interesting subject for future studies.

Acknowledgments

I thank Dr. Stanley A. Schumm and Dr. Ellen Wohl of Colorado State University for their comments on an

early draft of this manuscript. I also thank Dr. Teresa Ramirez of California State University, Long Beach, for her advice on my field work in California. This study was supported by the Grant-in-Aid for Scientific Research (C) (No. 13680107) from the Ministry of Education, Culture, Sports, Science and Technology, Japan, which is gratefully appreciated.

References

Allen, C.R., 1962. Circum-Pacific faulting in the Philippines–Taiwan region. Journal of Geophysical Research 67, 4795–4812.

Ando, K., 1972. Amount of stream-valley offset caused by strike-slip faulting in Miura and Izu Peninsulas and Yamazaki district. Geographical Review of Japan 45, 716–725 (in Japanese).

Benito, G., Pérez-González, A., Gutiérrez, F., Machade, M.J., 1998. River response to Quaternary subsidence due to evaporite solution (Gállego River, Ebro Basin, Spain). Geomorphology 22, 243–363.

Bull, W.L., 1997. Discontinuous ephemeral streams. Geomorphology 19, 227–276.

Bull, W.L., Knuepfer, P.L., 1987. Adjustments by the Charwell River, New Zealand, to uplift and climatic changes. Geomorphology 1, 15–32.

Burbank, D.J., Leland, J., Dumcan, C., 1996. Bedrock incision, rock uplift, and threshold hillslopes in the northwestern Himalayas. Nature 379, 505–510.

Burnett, A.W., Schumm, S.A., 1983. Alluvial-river response to neotectonic deformation in Louisiana and Mississippi. Science 222, 49–50.

Demoulin, A., 1998. Testing the tectonic significance of some parameters of longitudinal river profiles: the case of the Ardenne (Belgium, NW Europe). Geomorphology 24, 189–208.

Fukui, K., 1981. Fault topography along the Yamasaki fault system, western Kinki District, Japan. Geographical Review of Japan 54, 196–213 (in Japanese with English abstract).

Gaudemer, Y., Taponnere, P., Turcotte, D.L., 1989. River offsets across active strike-slip faults. Annales Tectonicae 3, 55–76.

Grant, L.B., Donnellan, A., 1994. 1855 and 1991 surveys of the San Andreas fault: implications for fault mechanics. Bulletin of the Seismological Society of America 84, 241–246.

Grant, L.B., Sieh, K.E., 1993. Stratigraphic evidence for seven meters of dextral slip on the San Andreas fault during the 1857 earthquake in the Carrizo Plain. Bulletin of the Seismological Society of America 83, 619–635.

Grant, L.B., Sieh, K.E., 1994. Paleoseismic evidence of clustered earthquakes on the San Andreas fault in the Carrizo Plain, California. Journal of Geophysical Research 99, 6819–6841.

Hack, J.T., 1957. Studies of longitudinal stream profiles in Virginia and Maryland. U.S. Geological Survey Professional Paper 294-B, 45–97.

Hack, J.T., 1973. Stream-profile analysis and stream-gradient index. Journal of Research of the U.S. Geological Survey 1, 421–429.

Harbor, D.J., 1998. Dynamic equilibrium between an active uplift and the Sevier River, Utah. Journal of Geology 106, 181–194.

Huang, H., 1993. Morphologic patterns of stream channels on the active Yishi Fault, southern Shandong Province, eastern China: implications for repeated great earthquakes in the Holocene. Tectonophysics 219, 283–304.

Kaneko, S., 1965. Transcurrent displacement along the Median Line, South-western Japan. New Zealand Journal of Geology and Geophysics 9, 45–59.

Keller, E.A., Rockwell, T.K., 1984. Tectonic geomorphology, Quaternary chronology and paleoseismicity. In: Costa, J.E., Fleicher, P.J. (Eds.), Development and Application of Geomorphology. Springer-Verlag, Berlin, pp. 203–239.

Keller, E.A., Bonkowski, M.S., Korsch, R.J., Shelemon, R.J., 1982. Tectonic geomorphology of the San Andreas fault zone in the southern Indio Hills, Coachella Valley, California. Geological Society of America Bulletin 93, 46–56.

Lawson, A.C., et al., 1908. The California Earthquake of April 18, 1906. Report of the State Earthquake Investigation Commission, I: Part1. The Carnegie Institution of Washington, Washington, DC. 254 pp.

Lensen, G.J., 1958. The Wellington fault from Cook Strait to Manawatu Gorge. New Zealand Journal of Geology and Geophysics 1, 178–196.

Matsuda, T., 1966. Strike-slip faulting along the Atotsugawa Fault, Japan. Bulletin of the Earthquake Research Institute 44, 1179–1212 (in Japanese with English abstract).

Matsuda, T., 1975. Active fault assessment for Irozaki fault system, Izu Peninsula. In: Tsuchi, R. (Ed.), Reports on the Earthquake Off the Izu Peninsula, 1974, and the Disaster. The Ministry of Education, Tokyo, pp. 121–125 (in Japanese).

McKeown, F.A., Jones-Cecil, M., Askew, B.L., McGrath, M.A., 1988. Analysis of stream profile data and inferred tectonic activity, eastern Ozark mountains region. U.S. Geological Survey Bulletin 1807, 1–39.

Merritts, D., Vincent, K.R., 1989. Geomorphic response of coastal streams to low, intermediate, and high rates of uplift, Mendocino triple junction region, northern California. Geological Society of America Bulletin 101, 1373–1388.

Okada, A., 1970. Fault topography and rate of faulting along the Median Tectonic Line in the drainage basin of the River Yoshino, northeastern Shikoku, Japan. Geographical Review of Japan 43, 1–21 (in Japanese with English abstract).

Okada, A., Sangawa, A., 1978. Fault morphology and Quaternary faulting along the Median Tectonic Line in the southern part of the Izumi Range. Geographical Review of Japan 51, 385–405.

Ouchi, S., 1985. Response of alluvial rivers to slow active tectonic movement. Geological Society of America Bulletin: 96, 504–515.

Ouchi, S., 2004. Flume experiments on the horizontal stream offset by a strike-slip fault. Earth Surface Processes and Landforms 29, 161–173.

Peterson, H.V., 1950. The problem of gullying in western valleys. In: Trask, P.D. (Ed.), Applied Sedimentation. John Wiley and Sons, New York, NY, pp. 407–434.

Rhea, S., 1989. Evidence of uplift near Charleston, South Carolina. Geology 17, 311–315.

Robertson, E.C., 1983. Relationship of fault displacement to gouge and breccia thickness. American Institute of Mining Engineering Transactions 274, 1426–1432.

Rockwell, T.K., Keller, E.A., Clark, M.N., Johnson, D.L., 1984. Chronology and rates of faulting of Venture River terraces, California. Geological Society of America Bulletin 95, 1466–1474.

Seeber, L., Gornitz, V., 1983. River profiles along the Himalayan Arc as indicators of active tectonics. Tectonophysics 92, 335–367.

Sieh, K.E., 1978. Slip along the San Andreas fault associated with the great 1857 earthquake. Bulletin of the Seismological Society of America 68, 1421–1448.

Sieh, K.E., 1984. Lateral offsets and revised dates of large prehistoric earthquakes at Pallett Creek, southern California. Journal of Geophysical Research 89, 7641–7670.

Sieh, K.E., Jahns, R.H., 1984. Holocene activity of the San Andreas fault at Wallace Creek, California. Geological Society of America Bulletin 95, 883–896.

Sieh, K.E., Stuiver, M., Brillinger, D., 1989. A more precise chronology of earthquakes produced by the San Andreas fault in southern California. Journal of Geophysical Research 94, 603–623.

Sims, J.D., Ito, T., Hamilton, J.C., Meier, D.B., 1989. Late Holocene record of earthquake and slip on the San Andreas fault in excavations on the Carrizo Plain, central California. Eos 70, 1349.

Snow, R.S., Slingerland, R.L., 1990. Stream profile adjustment to crustal warping. Nonlinear results from a simple model. Journal of Geology 98, 699–708.

Uemura, Y., 1988. Fault topography and Quaternary faulting of the Mitoke fault system in the southwestern part of the Tamba Highland, southwest Japan. Geographical Review of Japan 61-A, 453–468 (in Japanese with English abstract).

Wallace, R.E., 1968. Notes on stream channels offset by the San Andreas fault, Southern Coast Ranges, California. Stanford University Publications, Geological Sciences 11, 6–20.

Weldon, R.J., 1987. San Andreas fault, Cajon Pass, southern California. Geological Society of America Centennial Field Guide–Cordilleran Section, 193–198.

Weldon, R.J., Sieh, K.E., 1985. Holocene rare of slip and tentative recurrence interval for large earthquakes on the San Andreas fault, Cajon Pass, southern California. Geological Society of America Bulletin 96, 793–812.

Wells, S.G., Bullard, T.F., Menges, C.M., Drake, P.G., Karas, P.A., Kelson, K.I., Ritter, J.B., Wesling, J.R., 1988. Regional variations in tectonic geomorphology along a segmented convergent plate boundary, Pacific coast of Costa Rica. Geomorphology 1, 239–265.

Willemin, J.H., Knuepfer, L.K., 1994. Kinematics of arc-continent collision in the eastern Central Range of Taiwan inferred from geomorphic analysis. Journal of Geophysical Research 99, 20267–20280.

Yoshioka, T., 1986. Tectonic topography along the Hanaore fault in the northern Kinki District, Japan. Geographical Review of Japan 59, 191–204 (in Japanese with English abstract).

Zuchiewicz, W., 1995. Time-series analysis of river bed gradients in the Polish Carpathians: a statistical approach to the studies on young tectonic activity. Zeitschrift für Geomorphologie 39, 461–477.